

Electronic Supplementary Information

An ultra-fast synthesis of 13X@NaA composites through the plasma treatment for selective carbon capture

Jiali Huang,^a Jun Hu^{*a}, Wenli Du^b, Honglai Liu^a, Feng Qian^b, Meihong Wang^{*c}

^a Key Laboratory for Advanced Materials, School of Chemistry and Molecular Engineering, East China University of Science and Technology, 130 Meilong Road, Shanghai 200237, China. E-mail: junhu@ecust.edu.cn

Tel: +86 21 64252630.

^b School of Information Science and Engineering, East China University of Science and Technology, 130 Meilong Road, Shanghai 200237, China.

^c Department of Chemical and Biological Engineering, University of Sheffield, Sir Robert Hatfield Building, Mappin Street, Sheffield S1 3JD, UK. E-mail: Meihong.Wang@sheffield.ac.uk; Tel: +44 (0) 114 222 7160.

Figure captions

Scheme S1 Device of Dielectric Barrier Discharge.

Scheme S2 Schematic illustration of the synthesis approach of 13X@NaA.

Fig. S1 XRD patterns of 13X before and after the plasma treatment.

Fig. S2 XRD patterns of 13X@NaA composites with different plasma treatments after the crystallization aging for (a) 120 min (b) 60min (c) 15min; where * denotes the characteristic peaks of 13X, and ● denotes those of NaA.

Fig. S3 XRD pattern of the reference sample 13X@NaA composites after the crystallization aging for 6 h, where * denotes the characteristic peaks of 13X, and ● denotes those of NaA.

Fig. S4 Low magnification SEM micrographs of (a) bare 13X, (b) 13X@NaA-S-30, (c) 13X@NaA-N-60, (d) 13X@NaA-S-60, (e) 13X@NaA-S-120; high magnification SEM micrographs of (f) bare 13X, (g) 13X@NaA-S-30, (h) 13X@NaA-N-60, (i) 13X@NaA-S-60, (j) 13X@NaA-S-120.

Fig. S5 Effect of input power of the plasma treatment on the crystallinity of 13X@NaA-P.

Fig. S6 TGA curves of 13X before and after the plasma treatment under O₂ atmosphere.

Fig. S7 N₂ adsorption-desorption isotherms of 13X@NaA-S-30 and 13X@NaA-S-30 with different degrees of potassium ion exchange.

Fig. S8 CO₂ and N₂ adsorption isotherms at 298 K on 13X@NaA-S-120 with different degrees of potassium ion exchange.

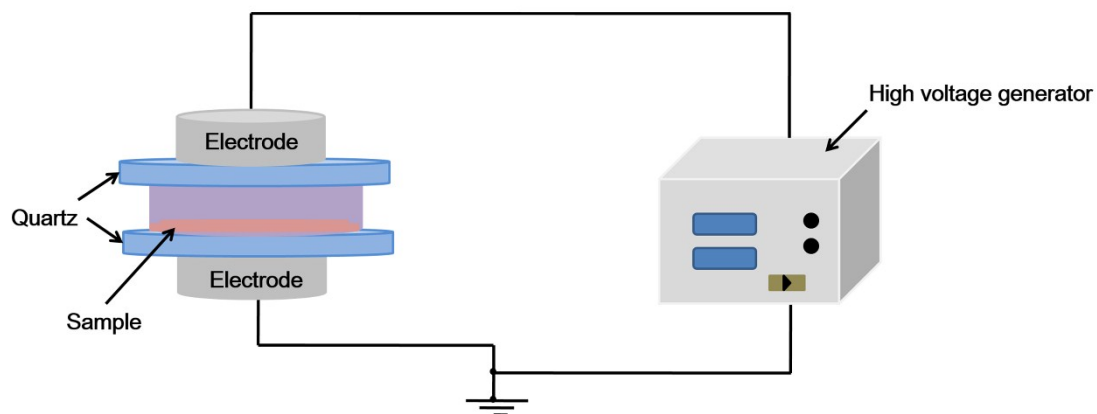
Fig. S9 (a) Dynamic CO₂ adsorption of 13X, 13X@NaA-S-30 and 13X@NaA-S-120 after potassium ion exchange at 323 K, (b) fitting plots of t/q_t against t as predicted by the second-order rate law.

Table S1 Changes of the relative crystallinity of NaA in 13X@NaA composite samples with the aging time and the input power of the plasma treatment.

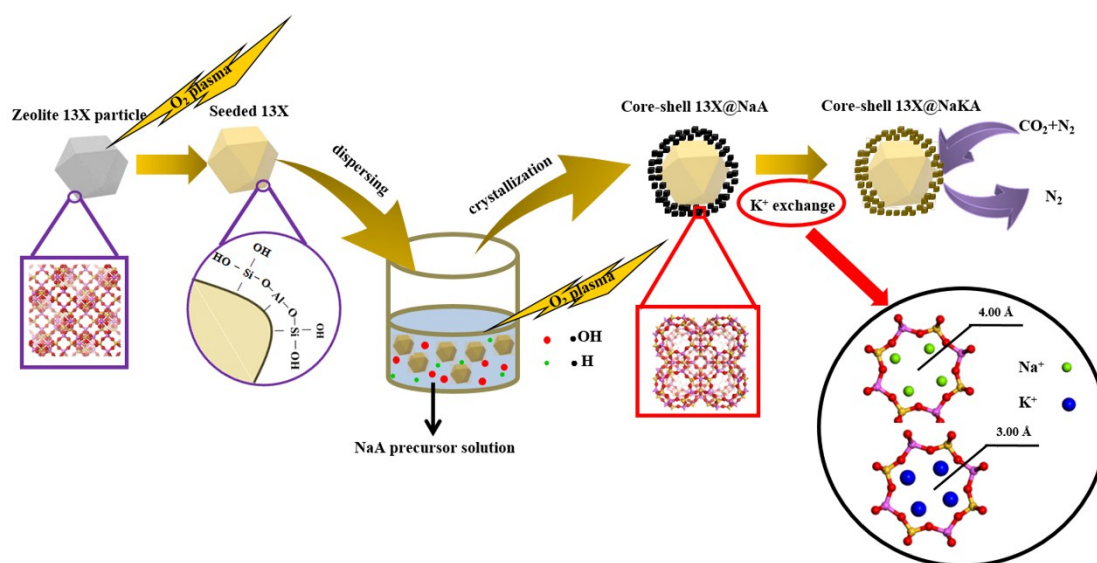
Table S2 CO₂ and N₂ uptakes, CO₂/N₂ selectivity of 13X, 13X@NaA-S-30 and 13X@NaA-S-120 with different potassium ion exchanges (collected at 298 K).

Table S3 Fitting parameters of the second-order kinetic model for CO₂ adsorption on 13X@NaA-S samples from the simulated flue gas at 298 K and 323 K.

Table S4 Comparison of CO₂ uptakes, CO₂/N₂ selectivity at 298 K (except for the specifications), and synthesis method with excellent state-of-the-art materials.



Scheme S1 Device of Dielectric Barrier Discharge.



Scheme S2 Schematic illustration of the synthesis approach of 13X@NaKA.

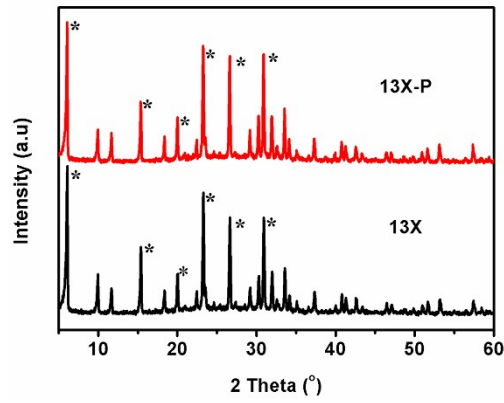


Fig. S1 XRD patterns of 13X before and after the plasma treatment.

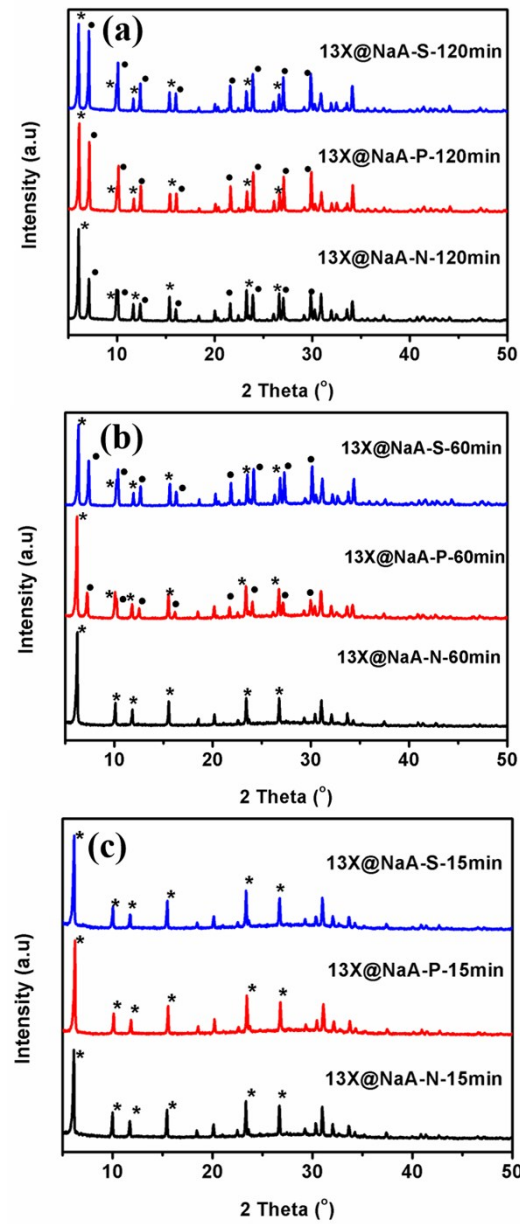


Fig. S2 XRD patterns of 13X@NaA composites with different plasma treatments after the crystallization aging for (a) 120 min (b) 60min (c) 15min; where * denotes the characteristic peaks of 13X, and • denotes those of NaA.

Calculation method of the relative crystallinity of NaA in 13X@NaA composites

Taking 13X@NaA powders which were produced by the traditional thermal crystallization route with ageing time of 6 h as the reference sample, in its XRD pattern (Fig. S3), the sum of integral peak intensities (R_s) of six characteristic (111) (210) (221) (311) (321) and (322) peaks of NaA in 11–32° two theta range was regarded as the criterion of 100% crystallinity. To eliminate the interference of the sample amount on the peak intensity, all XRD patterns of 13X@NaA composite samples were normalized by adjusting the intensity of (111) peak of 13X as the same as that of the standard 13X@NaA powders. Then, the sum of integral peak intensities (R_i) of six (111) (210) (221) (311) (321) and (322) peaks of NaA in the corresponding normalized XRD patterns of 13X@NaA composite samples was calculated, respectively. Comparing the intensity ratio R_i with the standard R_s , the relative crystallinity of NaA in all samples can be obtained. The recalculated results, as follows, were listed in Table S1, and the corresponding data in the discussion and Figs. 1(b), 1(d) and Fig. S5 were corrected in the revised manuscript.

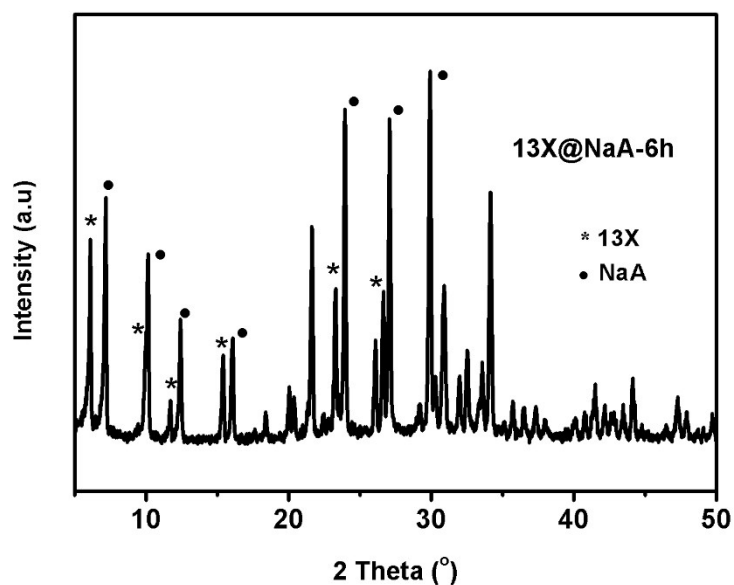


Fig. S3 XRD pattern of the reference sample 13X@NaA composites after the crystallization aging for 6 h, where * denotes the characteristic peaks of 13X, and ● denotes those of NaA.

Table S1 Changes of the relative crystallinity of NaA in 13X@NaA composite samples with the aging time and the input power of the plasma treatment.

Input Power (W) \ Aging time (min)	0	80	90	100
15	0	0	0	0
30	0	21.3 ^b /37.5 ^c	36.7 ^b /39.6 ^c	38.7 ^b /41.0 ^c
60	0	42.1 ^b /45.6 ^c	47.4 ^b /50.6 ^c	47.5 ^b /60.6 ^c
120	15.8 ^a	56.2 ^b /62.3 ^c	67.3 ^b /68.3 ^c	67.9 ^b /69.3 ^c

The relative crystallinity of NaA in ^a 13X@NaA-N, ^b 13X@NaA-P, and ^c 13X@NaA-S.

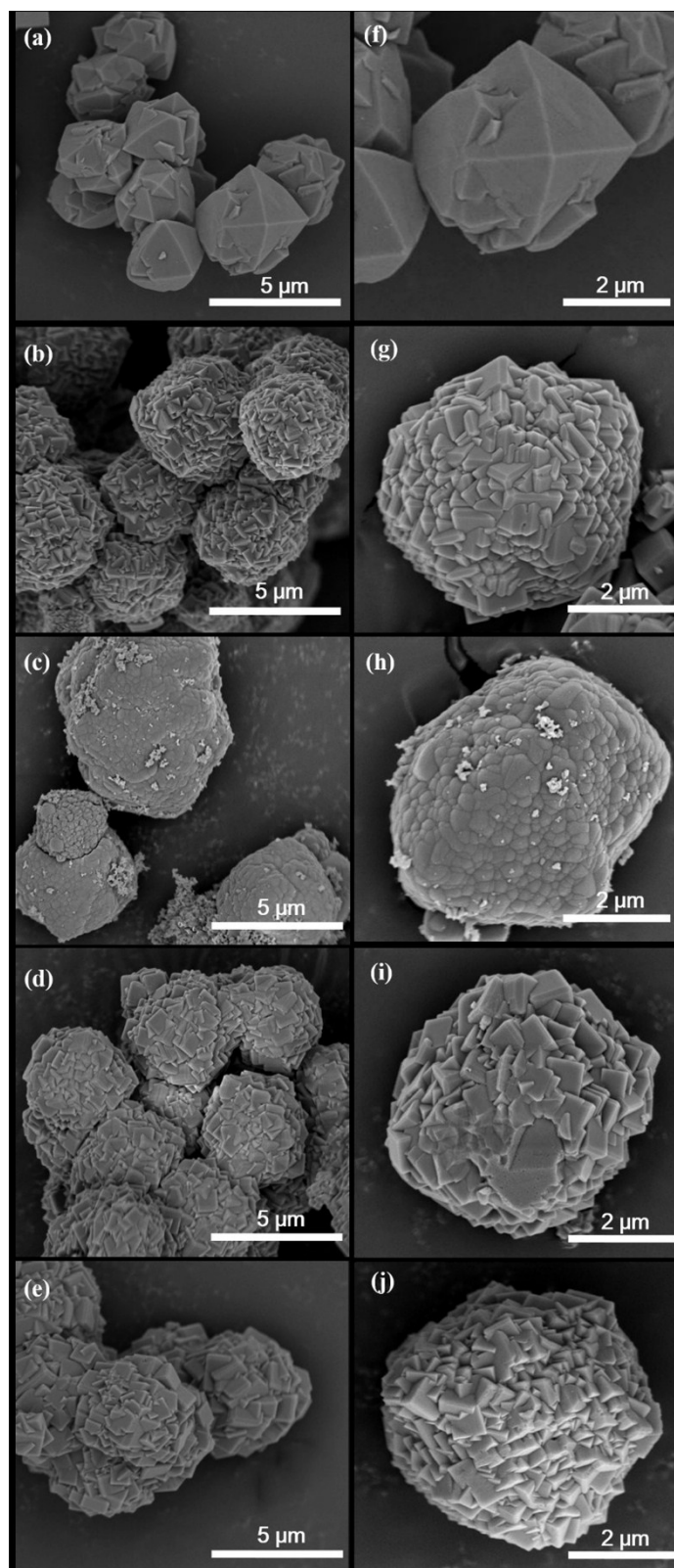


Fig. S4 Low magnification SEM micrographs of (a) bare 13X, (b) 13X@NaA-S-30, (c) 13X@NaA-N-60, (d) 13X@NaA-S-60, (e) 13X@NaA-S-120; high magnification SEM micrographs of (f) bare 13X, (g) 13X@NaA-S-30, (h) 13X@NaA-N-60, (i) 13X@NaA-S-60, (j) 13X@NaA-S-120.

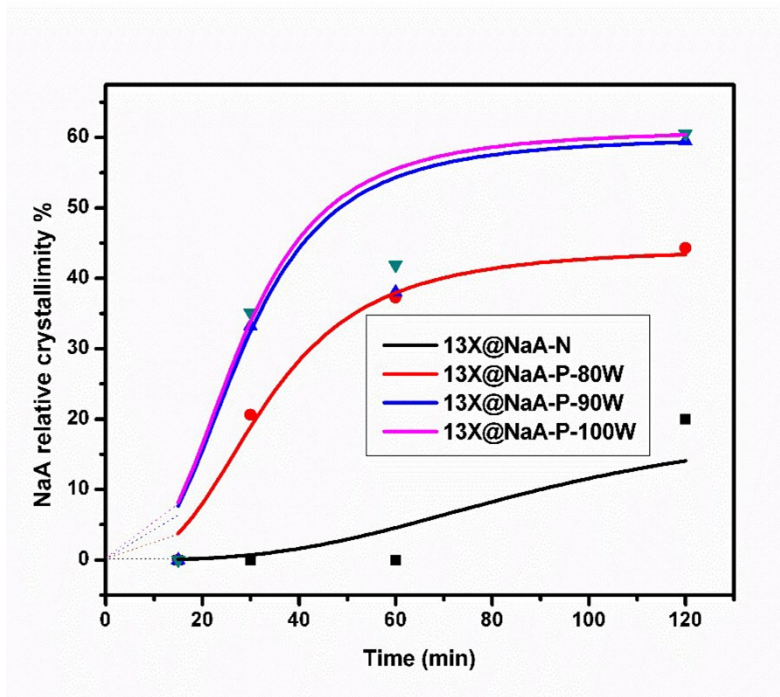


Fig. S5 Effect of input power of the plasma treatment on the crystallinity of 13X@NaA-P.

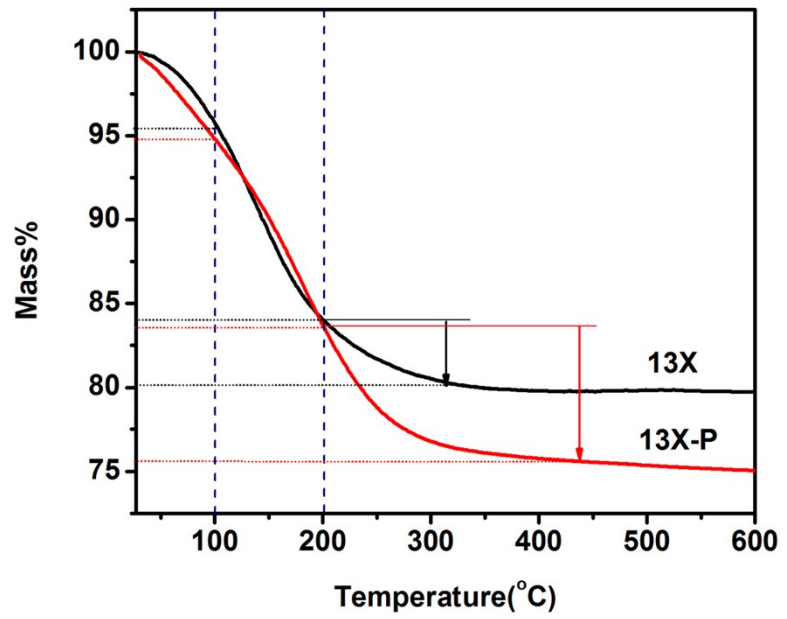


Fig. S6 TGA curves of 13X before and after the plasma treatment under O₂ atmosphere.

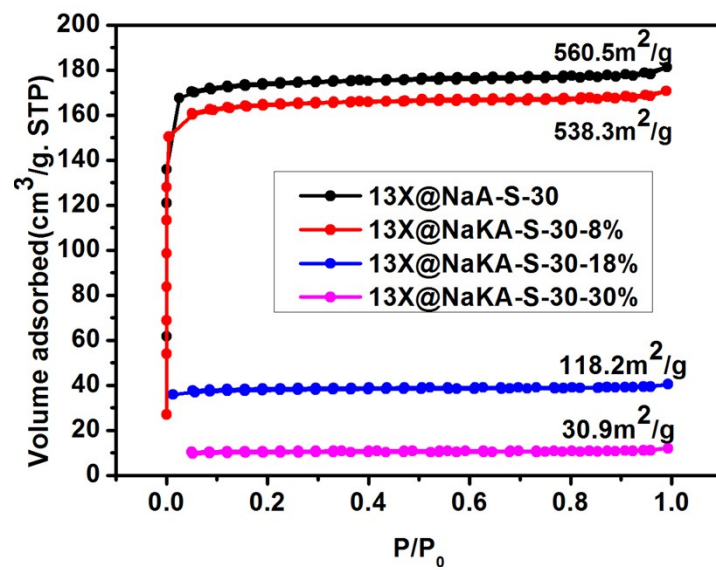


Fig. S7 N₂ adsorption-desorption isotherms of 13X@NaA-S-30 and 13X@NaKA-S-30 with different degrees of potassium ion exchange.

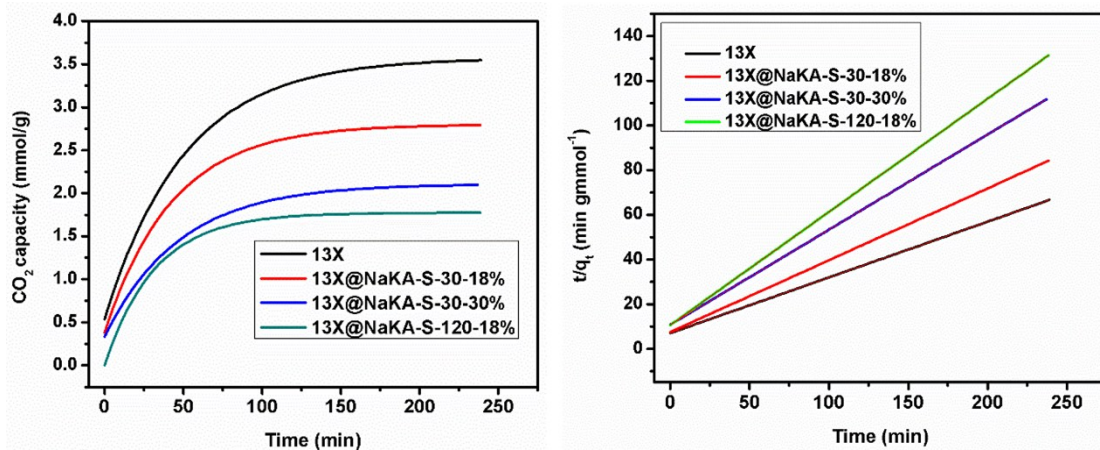


Fig. S9 (a) Dynamic CO₂ adsorption of 13X, 13X@NaKA-S-30 and 13X@NaKA-S-120 after potassium ion exchange at 323 K, (b) fitting plots of t/q_t against t as predicted by the second-order rate law.

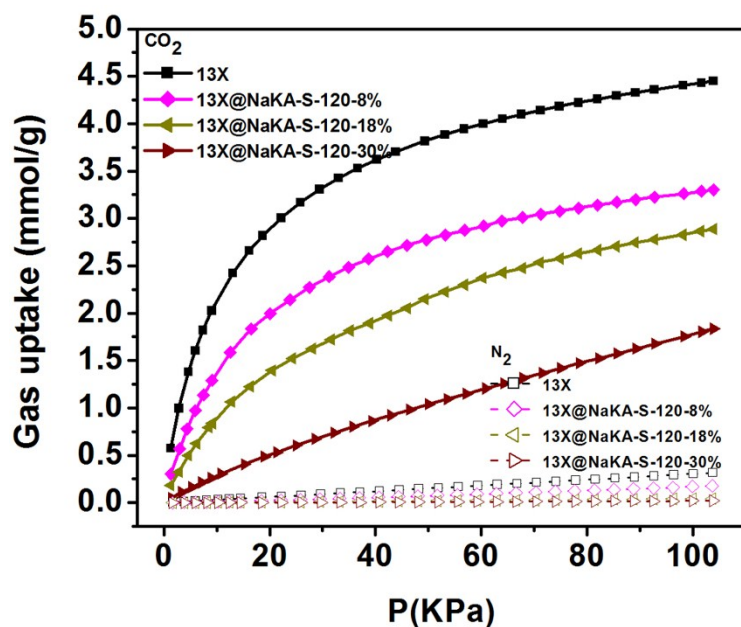


Fig. S8 CO₂ and N₂ adsorption isotherms at 298 K on 13X@NaA-S-120 with different degrees of potassium ion exchange.

Table S2 CO₂ and N₂ uptakes, CO₂/N₂ selectivity of 13X, 13X@NaA-S-30 and 13X@NaA-S-120 with different potassium ion exchanges (collected at 298 K).

Sample	CO ₂ uptake	N ₂ uptake	CO ₂ /N ₂
	[mmol g ⁻¹]	[mmol g ⁻¹]	selectivity
13X	4.45	0.32	60.3
13X@NaA-S-30	4.28	0.27	65.2
13X@NaKA-S-30-8%	4.07	0.20	78.6
13X@NaKA-S-30-18%	3.41	0.11	148.8
13X@NaKA-S-30-30%	2.60	0.03	280.5
13X@NaKA-S-120-8%	3.30	0.18	113.3
13X@NaKA-S-120-18%	2.89	0.04	264.4
13X@NaKA-S-120-30%	1.84	0.02	379.7

Table S3 Fitting parameters of the second-order kinetic model for CO₂ adsorption on 13X@NaKA-S samples from the simulated flue gas at 298 K and 323 K.

Sample	Rate constant k (g mmol ⁻¹ min ⁻¹)		Saturated uptakes q_e (mmol g ⁻¹)	
	298 K	323 K	298 K	323 K
13X	0.35	0.39	3.83	3.55
13X@NaKA-S-30-18%	0.22	0.25	2.95	2.80
13X@NaKA-S-30-30%	0.16	0.17	2.16	2.10
13X@NaKA-S-120-18%	0.10	0.11	1.97	1.80

Table S4 Comparison of CO₂ uptakes, CO₂/N₂ selectivity at 298 K (except for the specifications), and synthesis method with excellent state-of-the-art materials.

Type of sample	CO ₂ uptake at 298 K (mmol g ⁻¹)	CO ₂ /N ₂ selectivity	Synthesis method time	Ref.
NaK-ZK-4	2.50(293 K)	880(273 K)	Complicated synthesis about 120 h	36
Cu-SSZ-13/ H-SSZ-13	3.75/3.98	72.0 /73.6	Hydrothermal crystallization 144 h	38
azo-COP-2	1.53	130.6	Complicated synthesis about 25 h	39
azo-COP-10	1.15	165.2	Complicated synthesis about 25 h	40
PCBZL	1.24	148	Extensive Cross-Linking 24 h	
PCBZ	0.77	125	Oxidative Coupling Polymerization 24 h	41
P-PCz-3	5.76(273 K)	22	substituent effect controlling 49 h	42
PPF-1	6.07(273K)	14.5	Complicated synthesis about 72 h	43
NENU-520	2.71	400	Hydrothermal crystallization 72 h	44
Zn ₂ (C ₂ O ₄)(C ₂ N ₄ H ₃) ₂ •(H ₂ O) _x	2.70(303K)	98	Hydrothermal crystallization 48 h	45
PCN-88	7.14(273K)	23.1	Complicated synthesis 48 h	46

COF-TpAzo	1.56	145	Complicated synthesis about 76 h	47
3D-py-COF	3.72(273K)	22.5	Complicated synthesis about 96 h	48
13X@NaA-S-30	4.28	65.2	Plasma treatment -	
13X@NaKA-S-30-18%	3.41	148.8	Hydrothermal crystallization	
13X@NaKA-S-30-30%	2.60	280.5	30 min	This work
13X@NaKA-S-120-30%	1.84	379.7	Plasma treatment - Hydrothermal crystallization 120 min	